MORE TRAVELING WAVES IN THE HOLLING-TANNER MODEL WITH WEAK DIFFUSION

Vahagn Manukian [a,b] and Stephen Schecter [c]

[a] Department of Mathematics, Miami University, 301 S. Patterson Ave, Oxford, OH 45056, USA

[b] Department of Mathematical and Physical Sciences, Miami University, 1601 University Blvd, Hamilton, OH 45011, USA

[c] Department of Mathematics, North Carolina State University, Raleigh, NC 27695, USA

Abstract. We identify two new traveling waves of the Holling-Tanner model with weak diffusion. One connects two constant states; at one of them, the model is undefined. The other connects a constant state to a periodic wave train. We exploit the multi-scale structure of the Holling-Tanner model in the weak diffusion limit. Our analysis uses geometric singular perturbation theory, compactification and the blow-up method.

1. Introduction

In this paper we continue the study of traveling waves of the Holling-Tanner prey-predator model with weak diffusion, which was begun in [5]. We identify two types of traveling waves that were not considered in that paper. One connects two constant states; the novelty is that at one of the constant states, the origin, the model is undefined. The other connects a constant state to a periodic wave train.

1.1. **The model.** The diffusive Holling-Tanner prey-predator model is the reaction diffusion system

$$\begin{aligned} u_t &= D_u u_{xx} + u(1-u) - \frac{uv}{u+\alpha}, \\ v_t &= D_v v_{xx} + \delta v\left(1 - \frac{\beta v}{u}\right), \end{aligned} \tag{1.1}$$

In these equations, $t > 0$ is the time variable; $x \in \mathbb{R}$ is the spatial variable; D_u, D_v, α, δ and β are positive parameters. The quantity $u(x,t)$ is related to the prey population, and $v(x,t)$ is related to the predator population. Since physically meaningful solutions have u and v nonnegative, but the system (1.1) is undefined for $u = 0$, we consider (1.1) on the region $u > 0$, $v \geq 0$.

Date: May 8, 2020.

2010 *Mathematics Subject Classification.* 35B25, 35B32, 35K57, 35B36, 92D25.

Key words and phrases. geometric singular perturbation theory, traveling wave, compactification, prey-predator model, diffusive Holling-Tanner model, blow-up.

The spatially homogenous system

$$\begin{aligned} u_t &= u(1-u) - \frac{uv}{u+\alpha}, \\ v_t &= \delta v\left(1 - \frac{\beta v}{u}\right) \end{aligned} \tag{1.2}$$

associated with (1.1) is the Holling-Tanner model [7, 14, 15, 19, 16, 17]. In this model a predator captures prey at the rate $\frac{u}{u+\alpha}$, so there is a maximum rate which has been normalized to 1. The predator carrying capacity of the environment is $\frac{u}{\beta}$, i.e., it is proportional to the prey population u.

The bifurcation diagram of the ODE (1.2) has been elucidated in a series of papers [8, 6, 9, 10, 18]. We shall recall some of this work at various points in the paper. Turing bifurcations of the PDE (1.1) are studied in [13]. Existence of traveling front solutions that connect constant states of the PDE (1.1) has been established in [1, 2, 5], and existence of a family of wave train solutions was established in [5]. The importance of wave train solutions in ecological models is emphasized in [20].

1.2. **Equilibria.** Spatially homogeneous equilibria of the system (1.1) correspond to equilibria of (1.2). The system (1.2) has the three equilibria $(1,0)$, (u_+,v_+), (u_-,v_-), where

$$u_\pm = \frac{\beta(1-\alpha) - 1 \pm \sqrt{(\beta(1-\alpha)-1)^2 + 4\alpha\beta^2}}{2\beta} \quad \text{and } v_\pm = \frac{1}{\beta}u_\pm. \tag{1.3}$$

Since u_+ and v_+ are positive, but u_- and v_- are negative, we shall consider the equilibrium (u_+,v_+) but ignore (u_-,v_-). We let $A=(u_+,v_+)$ and $B=(1,0)$.

The equilibrium A is the rightmost intersection of the parabola $v=(1-u)(u+\alpha)$ and the line $v=(1/\beta)u$. The parabola opens downward and has vertex $V=((1-\alpha)/2, ((1+\alpha)^2/4)$.

We define two regions of $\alpha\beta$-parameter space,

$$\mathcal{R}_1 = \{(\alpha,\beta) : 0<\alpha<1 \text{ and } \beta > \frac{2(1-\alpha)}{(\alpha+1)^2}\} \cup \{(\alpha,\beta) : \alpha \geq 1 \text{ and } \beta > 0\},$$

and

$$\mathcal{R}_2 = \{(\alpha,\beta) : 0<\alpha<1 \text{ and } 0<\beta < \frac{2(1-\alpha)}{(\alpha+1)^2}\}.$$

In $\mathcal{R}_1$, A lies to the right of V. In $\mathcal{R}_2$, V is in the first quadrant, and A lies to the left of V.

The second equation of (1.2) is not defined at $u=0$; however, if we multiply the system (1.2) by u, another equilibrium appears, at $O=(0,0)$. Although the systems (1.1) and (1.2) are undefined at O, this point is nevertheless of interest, since it represents the state at which both populations are zero.

1.3. **Traveling waves.** To find traveling waves with velocity c, we rewrite the system (1.1) in a frame that is moving with velocity c, i.e., we make the change of variables $\zeta = x - ct$. In addition we introduce the ratio $\mu = D_v/D_u$. We obtain

$$\begin{aligned} u_t &= D_u u_{\zeta\zeta} + cu_\zeta + u(1-u) - \frac{uv}{u+\alpha}, \\ v_t &= \mu D_u v_{\zeta\zeta} + cv_\zeta + \delta v\left(1 - \frac{\beta v}{u}\right). \end{aligned} \tag{1.4}$$

Traveling waves of (1.1) with velocity c correspond to stationary solutions of (1.4). We consider only traveling waves with nonzero velocity.

It turns out that traveling waves exist for any $c \neq 0$. It is therefore convenient to introduce the scaling $z = \zeta/c$, so (1.4) becomes

$$\begin{aligned} u_t &= \frac{D_u}{c^2} u_{zz} + u_z + u(1-u) - \frac{uv}{u+\alpha}, \\ v_t &= \frac{D_u}{c^2}\mu\, v_{zz} + v_z + \delta v\left(1 - \frac{\beta v}{u}\right). \end{aligned} \tag{1.5}$$

Finally we set $\epsilon = D_u/c^2$ to obtain

$$\begin{aligned} u_t &= \epsilon u_{zz} + u_z + u(1-u) - \frac{uv}{u+\alpha}, \\ v_t &= \epsilon\mu\, v_{zz} + v_z + \delta v\left(1 - \frac{\beta v}{u}\right). \end{aligned} \tag{1.6}$$

A stationary solution of (1.6) corresponds, for a given $D_u > 0$ and $c \neq 0$ with $\epsilon = D_u/c^2$, to a stationary solution of (1.4), and hence to a traveling wave of (1.1) with $D_v = \mu D_u$ and velocity c.

We assume $\epsilon \ll 1$, i.e., $D_u \ll c^2$. Thus diffusion is very slow compared to the speed of the wave.

Stationary solutions of (1.6) correspond to solutions of the traveling wave ODE system

$$\begin{aligned} 0 &= \epsilon u_{zz} + u_z + u(1-u) - \frac{uv}{u+\alpha}, \\ 0 &= \epsilon\mu v_{zz} + v_z + \delta v\left(1 - \frac{\beta v}{u}\right), \end{aligned} \tag{1.7}$$

1.4. **Results.** In [5] the following results are shown.

Theorem 1.1. *Assume (1)* (α, β) *is in* $\mathcal{R}_1$, $\mu > 0$, *and* $\delta > 0$, *or (2)* (α, β) *is in* $\mathcal{R}_2$, $\mu > 0$, *and* $\delta > 1 - \alpha$. *Then for sufficiently small* $\epsilon > 0$, *there is a positive solution* $(u(z), v(z))$ *of* (1.7) *that satisfies the boundary conditions*

$$\lim_{z\to-\infty} (u(z), v(z)) = A, \tag{1.8}$$

$$\lim_{z\to+\infty} (u(z), v(z)) = B, \tag{1.9}$$

The solution is unique up to a shift in z.

The solution of Theorem 1.1 corresponds to a traveling front of (1.1) that connects the equilibria A and B. The state A, in which predator and prey coexist, gradually expands in space to replace the state B, in which only the prey is present.

Theorem 1.2. *Assume (α, β) is in $\mathcal{R}_2$, $\mu > 0$, and $\delta > 0$ is sufficiently small. Then for sufficiently small $\epsilon > 0$, there is a positive periodic solution $(u(z), v(z))$ of (1.7).*

The periodic solution of Theorem 1.2 corresponds to a wave train of (1.1).

In this paper we shall prove the following results, which extend the above theorems.

Theorem 1.3. *Assume (α, β) is in $\mathcal{R}_1$ or $\mathcal{R}_2$, $\mu > 0$, and $\delta > 1$. Then for sufficiently small $\epsilon > 0$, there is a 2-parameter family of positive solutions $(u(z), v(z))$ of (1.7), defined for all z, that satisfy the boundary conditions*

$$\lim_{z \to -\infty} (u(z), v(z)) = A, \tag{1.10}$$

$$\lim_{z \to +\infty} (u(z), v(z)) = O, \tag{1.11}$$

One of the parameters in Theorem 1.3 of course represents shifts in the traveling waves. We specify that the solutions are defined for all z since *a priori* solutions that approach O, where the system is undefined, could do so in finite time.

The solutions of Theorem 1.3 correspond to traveling fronts of (1.1) that connect the equilibrium A to the point O. The state A, in which predator and prey coexist, gradually expands in space to replace the state O, in which both predator and prey are absent.

Theorem 1.4. *Assume (α, β) is in $\mathcal{R}_2$, $\mu > 0$, $\delta > 0$, $\beta\delta \neq 2$, and there exists a hyperbolic positive closed orbit of the traveling wave system (1.7). Then for sufficiently small $\epsilon > 0$, there is a positive solution $(u(z), v(z))$ of (1.7) that connects a periodic solution at $z = -\infty$ to the constant state B at $z = \infty$.*

Positive closed orbits of (1.7) must surround A. By Theorem 1.2, such orbits exist at least for small δ, and they cannot exist for $\delta > 1 - \alpha$. We discuss the interval of existence further in Sec 3.

The solutions of Theorem 1.4 correspond to traveling waves of (1.1) that connect a wave train to the point B. The wave train, in which predator and prey populations oscillate, gradually expands in space to replace the state B, in which only the prey is present.

The remainder of the paper is devoted to the proofs of Theorems 1.3 and 1.4. We shall always assume that the parameters α, β, μ and δ are positive, and shall indicate where further assumptions on (α, β) and δ are required.

2. First-order system, rescaling, blow-up, and proof of Theorem 1.3

2.1. **First-order system.** We set

$$(u, u_1, v, v_1) = (u, \frac{du}{dz}, v, \frac{du}{dz})$$

and rewrite (1.7) as the first-order system

$$\begin{aligned}
\frac{du}{dz} &= u_1, \\
\epsilon\frac{du_1}{dz} &= -u_1 - u(1-u) + \frac{uv}{u+\alpha}, \\
\frac{dv}{dz} &= v_1, \\
\epsilon\frac{dv_1}{dz} &= -\frac{1}{\mu}v_1 - \frac{\delta}{\mu}v\left(1-\frac{\beta v}{u}\right).
\end{aligned} \tag{2.1}$$

System (2.1) is known as the slow system in geometric singular perturbation theory. The corresponding fast system is obtained by setting $z = \epsilon\xi$:

$$\begin{aligned}
\frac{du}{d\xi} &= \epsilon u_1, \\
\frac{du_1}{d\xi} &= -u_1 - u(1-u) + \frac{uv}{u+\alpha}, \\
\frac{dv}{d\xi} &= \epsilon v_1, \\
\frac{dv_1}{d\xi} &= -\frac{1}{\mu}v_1 - \frac{\delta}{\mu}v\left(1-\frac{\beta v}{u}\right).
\end{aligned} \tag{2.2}$$

2.2. **Blow-up at the origin.** We will work with the fast system (2.2). In order to see solutions of (2.2) near the origin more clearly, we use the blow-up coordinates

$$u_1 = Pu, \quad v = Qu, \quad v_1 = Ru$$

in (2.2). Note that this will convert the term $\frac{v}{u}$ in the fourth equation of (2.2) to Q. In order to have a polynomial system, which will be convenient in Sec. 3, we multiply the resulting vector field by $u+\alpha$. Equivalently, we make the change of independent variable

$$\eta = \int_0^\xi \frac{1}{u(s)+\alpha}\,ds,$$

which makes sense as long as $u(s) > -\alpha$. We obtain

$$\begin{aligned}
\frac{du}{d\eta} &= \epsilon Pu(u+\alpha), \\
\frac{dP}{d\eta} &= -\epsilon P^2(u+\alpha) - P(u+\alpha) + u^2 + (Q+\alpha-1)u - \alpha, \\
\frac{dQ}{d\eta} &= \epsilon(R-PQ)(u+\alpha), \\
\frac{dR}{d\eta} &= -\frac{1}{\mu}(u+\alpha)(\epsilon\mu PR - \beta\delta Q^2 + \delta Q + R).
\end{aligned} \tag{2.3}$$

Setting $\epsilon = 0$ in (2.3), we obtain

$$\begin{aligned}\frac{du}{d\eta} &= 0,\\ \frac{dP}{d\eta} &= -P(u+\alpha) + u^2 + (Q+\alpha-1)u - \alpha,\\ \frac{dQ}{d\eta} &= 0,\\ \frac{dR}{d\eta} &= \frac{1}{\mu}(u+\alpha)(\beta\delta Q^2 - \delta Q - R).\end{aligned} \tag{2.4}$$

In $u \geq 0$ the set of equilibria of (2.4) is the two-dimensional manifold

$$\mathcal{M}_0 = \left\{(u,P,Q,R) :\ P = \frac{Qu + \alpha u + u^2 - \alpha - u}{u+\alpha},\ R = \beta\delta Q^2 - \delta Q, u \geq 0\right\}, \tag{2.5}$$

the critical manifold of (2.3) in $u \geq 0$. Linearizing (2.4) about each point of $\mathcal{M}_0$, we find two zero eigenvalues and two negative eigenvalues $-(u+\alpha)$ and $-(u+\alpha)/\mu$, so $\mathcal{M}_0$ is normally hyperbolic and attracting for the system (2.4).

By Fenichel's First Theorem [4, 11, 12], any compact subset of $\mathcal{M}_0$ perturbs, for small $\epsilon > 0$, to a manifold

$$\mathcal{M}_\epsilon = \mathcal{M}_0 + \mathrm{O}(\epsilon)$$

that is invariant under (2.3), normally hyperbolic, and attracting.

The slow system corresponding to (2.3) is obtained by setting $w = \epsilon\eta$:

$$\begin{aligned}\frac{du}{dw} &= u(u+\alpha)P,\\ \epsilon\frac{dP}{dw} &= -\epsilon P^2(u+\alpha) - P(u+\alpha) + u^2 + (Q+\alpha-1)u - \alpha,\\ \frac{dQ}{dw} &= (R - PQ)(u+\alpha),\\ \epsilon\frac{dR}{dw} &= -\frac{1}{\mu}(u+\alpha)(\epsilon\mu PR - \beta\delta Q^2 + \delta Q + R).\end{aligned} \tag{2.6}$$

The reduced slow system on $\mathcal{M}_0$ is obtained by substituting the equations for P and R in (2.5) into (2.6) and setting $\epsilon = 0$:

$$\begin{aligned}\frac{du}{dw} &= u(u^2 + (Q+\alpha-1)u - \alpha),\\ \frac{dQ}{dw} &= Q\left((\beta\delta Q - \delta)(u+\alpha) - (u^2 + (Q+\alpha-1)u - \alpha)\right).\end{aligned} \tag{2.7}$$

The slow system on $\mathcal{M}_\epsilon$ is a perturbation of (2.7):

$$\begin{aligned}\frac{du}{dw} &= u((u^2 + (Q+\alpha-1)u - \alpha) + \mathrm{O}(\epsilon)),\\ \frac{dQ}{dw} &= Q\left((\beta\delta Q - \delta)(u+\alpha) - (u^2 + (Q+\alpha-1)u - \alpha)\right) + \mathrm{O}(\epsilon).\end{aligned} \tag{2.8}$$

2.3. **The reduced slow system** (2.7) **on** $\mathcal{M}_0$**.** For the reduced slow system (2.7), both axes are invariant. There are four equilibria in $u \geq 0$: $K = (0,0)$, $L = (0, \frac{\delta-1}{\beta\delta})$, $\tilde{B} = (1,0)$, and $\tilde{A} = (u_+, Q_+)$, with

$$\begin{aligned} u_+ &= \frac{1}{2\beta}\left((1-\alpha)\beta - 1 + \sqrt{((1-\alpha)\beta-1)^2 + 4\alpha\beta^2}\right), \\ Q_+ &= \frac{1}{\beta}. \end{aligned}$$

The points $\tilde{B}$ and $\tilde{A}$ correspond to B and A, defined earlier, in uv-coordinates. The line $u = 0$ in uQ-space, including the points K and L, corresponds to the origin O in uv-coordinates.

For the system (2.7):

(i) The equilibrium K has the eigenvalues $-\alpha$ and $-\alpha(\delta-1)$. It is therefore a hyperbolic saddle for $\delta < 1$ and a hyperbolic attractor for $\delta > 1$.
(ii) The equilibrium L has a positive (resp. negative) B-coordinate for $\delta > 1$ (resp. for $\delta < 1$). It has the eigenvalues $-\alpha$ and $\alpha(\delta - 1)$. It is therefore a hyperbolic saddle for $\delta > 1$ (resp. a hyperbolic attractor for $\delta < 1$).
(iii) The equilibrium $\tilde{B}$ has the eigenvalues $1 + \alpha$ and $-\delta(1 + \alpha)$. It is therefore a hyperbolic saddle .

The nature of the equilibrium $\tilde{A}$ is less evident. However, a calculation shows:

Proposition 2.1. *If we make the change of variables $v = Qu$ in the spatially homogenous system* (1.2)*, then multiply the resulting system by $-(u + \alpha)$, we obtain the reduced slow system* (2.7)*. The system* (1.2) *in the region $u > 0$, $v \geq 0$, with time reversed, is therefore smoothly equivalent to the system* (2.7) *in the region $u > 0$, $Q \geq 0$.*

Therefore the nature of the equilibrium $\tilde{A}$ in (2.7) follows from the nature of the corresponding equilibrium A in (1.2). Using Propositions 4.1 and 5.1 of [5] we obtain:

(i) For (α, β) in $\mathcal{R}_1$ and $\delta > 0$, the equilibrium $\tilde{A}$ is a hyperbolic repeller of (2.7).
(ii) For (α, β) is in $\mathcal{R}_2$ there exists δ_h with $0 < \delta_h < 1 - \alpha$ such that the equilibrium $\tilde{A}$ is a hyperbolic attractor of (2.7) for $0 < \delta < \delta_h$, and a hyperbolic repeller of (2.7) for $\delta_h < \delta < \infty$. A Hopf bifurcation occurs at $\delta = \delta_h$.

See Figure 2.1.

2.4. **The slow system** (2.8) **on** $\mathcal{M}_\epsilon$**.** Since the equilibria $K = (0,0)$, $L = (0, \frac{\delta-1}{\beta\delta})$, $\tilde{B} = (1,0)$, and $\tilde{A} = (u_+, B_+)$ of the reduced slow system (2.7) are hyperbolic, the slow system (2.8) has nearby equilibria K_ϵ, L_ϵ, $\tilde{B}_\epsilon$, and $\tilde{A}_\epsilon$ of the same types.

Proposition 2.2. *For any sufficiently small $\epsilon > 0$, the line $u = 0$ is invariant under the slow system* (2.8) *on $\mathcal{M}_\epsilon$, and contains K_ϵ and L_ϵ.*

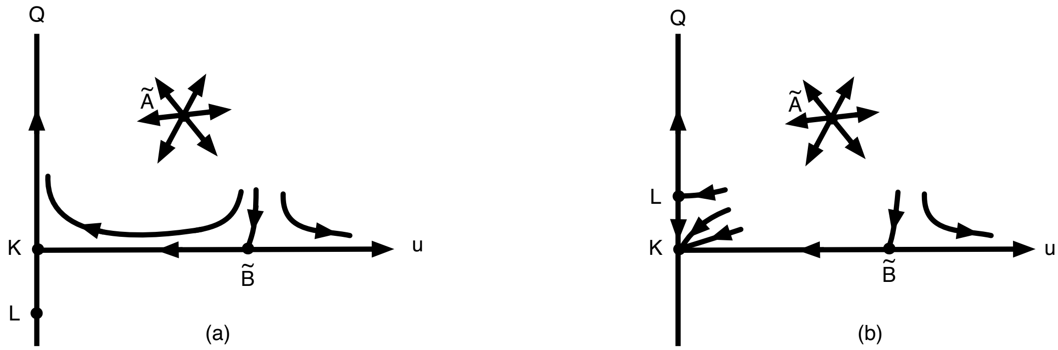

FIGURE 2.1. Equilibria of (2.7): (a) $0 < \delta < 1$,(b) $\delta > 1$. The equilibrium $\tilde{A}$ is pictured as a repeller, which is correct for (α, β) is in $\mathcal{R}_1$, and for (α, β) in $\mathcal{R}_2$ provided $\delta_h < \delta < \infty$, where $0 < \delta_h < 1 - \alpha$.

Proof. Invariance follows from the fact that for the full slow system (2.6), the 3-dimensional space $u = 0$ is invariant for any ϵ. Since K and L are hyperbolic within $u = 0$ for the reduced slow system (2.7) on $\mathcal{M}_0$, it follows that K_ϵ and L_ϵ are contained in $u = 0$. □

Proposition 2.3. *For any sufficiently small $\epsilon > 0$, K_ϵ and $\tilde{B}_\epsilon$ are contained in the line $Q = 0$. In addition, the portion of the line $Q = 0$ that lies between K_ϵ and $\tilde{B}_\epsilon$ is invariant under the slow system* (2.8) *on $\mathcal{M}_\epsilon$.*

Proof. Note that for the full slow system (2.6), the 2-dimensional space $Q = R = 0$ is invariant for any ϵ. Within this space, for $\epsilon = 0$ there is a curve $\mathcal{C}_0$ of equilibria given by $P = \frac{\alpha u + u^2 - \alpha - u}{u + \alpha}$ (compare (2.5)). $\mathcal{C}_0$ is a normally hyperbolic curve of equilibria within $Q = R = 0$. It therefore perturbs to a normally hyperbolic invariant curve $\mathcal{C}_\epsilon$ within $Q = R = 0$. Since K and L are hyperbolic equilibria within $\mathcal{C}_\epsilon$ for the reduced slow system, it follows that $\mathcal{C}_\epsilon$ includes K_ϵ and $\tilde{B}_\epsilon$.

We cannot immediately conclude that $\mathcal{C}_\epsilon$ is part of $\mathcal{M}_\epsilon$, due to nonuniqueness of perturbations of the normally hyperbolic invariant manifolds $\mathcal{M}_0$. However, $\mathcal{M}_\epsilon$ must include all nearby bounded orbits. Therefore $\mathcal{M}_\epsilon$ includes K_ϵ, $\tilde{B}_\epsilon$, and the portion of $\mathcal{C}_\epsilon$ between them, which is a bounded orbit. This implies that under the slow system (2.8) on $\mathcal{M}_\epsilon$, the portion of the line $Q = 0$ that lies between K_ϵ and $\tilde{B}_\epsilon$ is invariant. □

Proposition 2.4. *$K_\epsilon = K$, $L_\epsilon = (0, \frac{\delta - 1}{\beta\delta} + \mathcal{O}(\epsilon))$, $\tilde{B}_\epsilon = B$, and $\tilde{A}_\epsilon = A$.*

Proof. By the previous propositions, K_ϵ is contained in both $u = 0$ and $Q = 0$. Therefore $K_\epsilon = K$.

Using (2.5), L, $\tilde{B}$, and $\tilde{A}$ correspond respectively to the following equilibria of (2.4):

$$(0,-1,\frac{\delta-1}{\beta\delta},\ \frac{1-\delta}{\beta\delta}),\ (1,0,0,0),\ (u_+,0,B_+,0).$$

The last two are equilibria of (2.3) for any ϵ; therefore $\tilde{B}_\epsilon = B$ and $\tilde{A}_\epsilon = A$. The first is not an equilibrium of (2.3) for $\epsilon \neq 0$. (The problem is the term $-\epsilon P^2(u+\alpha)$ in the second equation.) However, L_ϵ has the given form by Proposition 2.2. □

2.5. **Proof of Theorem 1.3.** The following result is stated in [5]; it is a reformulation of a result in [8].

Lemma 2.5. *If* (α,β) *is in* $\mathcal{R}_1$ *and* $\delta > 0$*, or* (α,β) *is in* $\mathcal{R}_2$ *and* $\delta > 1-\alpha$*, then* A *is a global attractor of* (1.2) *in the region* $u > 0$*,* $v > 0$*.*

We now prove Theorem 1.3.

For the reduced slow system (2.7) on $\mathcal{M}_0$ and $\delta > 1$, we consider in Figure 2.1 (b) the open one-parameter family $\mathcal{F}_0$ of orbits that approach the attractor K as time increases, bounded on one side by a connection along the vertical axis from the saddle L to K, and on the other side by a connection along the horizontal axis from the saddle $\tilde{B}$ to K.

From Lemma 2.5 and Proposition 2.1, the orbits in $\mathcal{F}$, along with the stable manifolds of L and $\tilde{B}$, approach $\tilde{A}$ in backward time.

For small $\epsilon > 0$, we consider the slow system (2.8) on $\mathcal{M}_\epsilon$. The Q-axis, and the u-axis between K and $\tilde{B}_\epsilon$, remain invariant by Propositions 2.2 and 2.3, and the equilibria perturb as described in Proposition 2.4. There is a connection from the saddle L_ϵ to the attractor K along the vertical axis, and a connection from the saddle $\tilde{B}$ to K along the horizontal axis. In addition, the stable manifolds of L_ϵ and $\tilde{B}$ approach $\tilde{A}$ in backward time.

We consider the open one-parameter family of orbits $\mathcal{F}_\epsilon$ that approach K_ϵ as time increases, bounded by the connections from L_ϵ and $\tilde{B}$ to K. It follows from the previous paragraph that these orbits approach $\tilde{A}$ in backward time.

After blow-down from $uPQR$-coordinates to uu_1vv_1 coordinates, the family $\mathcal{F}_\epsilon$ corresponds to a one-parameter family $\mathcal{G}_\epsilon$ of orbits of (2.2) that connect $(u_+,0,v_+,0)$ to $(0,0,0,0)$. The orbits in $\mathcal{G}_\epsilon$ correspond to the traveling wave solutions of (1.7) described in the theorem. They are positive ($u > 0$ and $v > 0$) since for the orbits in $\mathcal{F}_\epsilon$, $u > 0$ and $Q > 0$. They are defined for infinite time, since the orbits in $\mathcal{F}_\epsilon$ are defined for infinite time, and the various changes of independent variable do not affect this property.

3. Poincaré sphere and proof of Theorem 1.4

Figure 3.1, which is based on Figure 2.1(a), shows equlibria and closed orbits of (2.7) when positive closed orbits are present. There may be several closed orbits surrounding $\tilde{A}$. We must have (α,β) in $\mathcal{R}_2$ and $0 < \delta \leq 1-\alpha$, since $\tilde{A}$ is a global repeller of (2.7) for (α,β) in $\mathcal{R}_1$ and for (α,β) in $\mathcal{R}_2$ with $1-\alpha < \delta < \infty$ (Lemma 2.5 and Proposition 2.1).

We remark that for (α, β) in $\mathcal{R}_2$, a family of large closed orbits of relaxation type appears for small $\delta > 0$ in a global bifurcation [5]. As mentioned in Subsec. 2.3, a Hopf bifurcation occurs at $\delta = \delta_h$ with $0 < \delta_h < 1 - \alpha$. According to [18], when this bifurcation is subcritical, the family of closed orbits dies in the Hopf bifurcation; when it is supercritical, the family turns at a value of δ with $\delta_h < \delta \leq 1 - \alpha$ and then dies in the Hopf bifurcation.

To prove Theorem 1.4 we shall show that under the hypotheses of the theorem, for the system (2.7), the stable manifold of the saddle $\tilde{B}$ approaches the outermost closed orbit in backward time. It follows that for small $\epsilon > 0$, the stable manifold of the saddle $\tilde{B}$ is bounded in backward time. Since by assumption at least one of the closed orbits of (2.7) that surrounds $\tilde{A}$ is hyperbolic, it also persists for for small $\epsilon > 0$. The result follows.

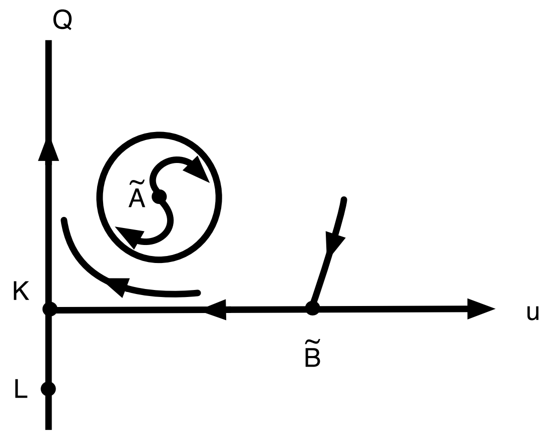

FIGURE 3.1. Equilibria and positive closed orbits of (2.7) when positive closed orbits are present. There may be several closed orbits surrounding $\tilde{A}$. We must have (α, β) in $\mathcal{R}_2$ and $0 < \delta \leq 1 - \alpha$.

To show that under the hypotheses of the theorem, for the system (2.7), the stable manifold of the saddle $\tilde{B}$ approaches the outermost closed orbit in backward time, it suffices to show that it does not go to infinity in backwards time. To show this we shall compactify the phase space of (2.7) by adding a circle at infinity. In other words, we look at the flow on the Poincaré sphere. This approach is also used in [18], for the system (1.2) multiplied by $u(u + \alpha)$, although details are not given there.

It turns out that there are two cases, depending on whether $\beta\delta < 2$ or $\beta\delta > 2$; see Figure 3.2. In both cases there are equilibria on the circle at infinity, but those in the first quadrant, which is invariant, do not attract any orbits in the finite plane in backwards time. Therefore the stable manifold of the saddle $\tilde{B}$ does not go to infinity in backwards time.

The remainder of this section is devoted to justifying Figure 3.2.

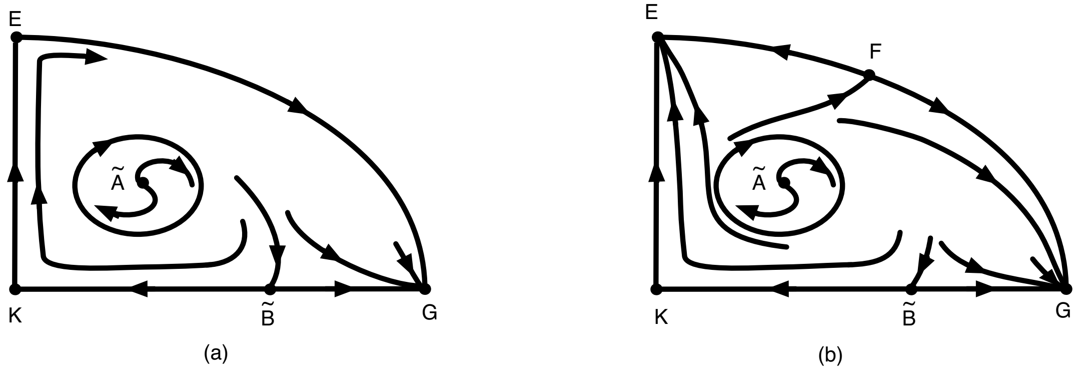

FIGURE 3.2. The flow in the quadrant $X \geq 0,\ Y \geq 0$ of the Poincaré sphere when positive closed orbits are present: (a) $\beta\delta < 2$, (b) $\beta\delta > 2$.

3.1. **Poincaré sphere.** For the analysis in this section we find it more convenient and aesthetically pleasing to rewrite (2.7) as

$$\begin{aligned} u' &= u^3 + (v+\alpha-1)u^2 - \alpha u, \\ v' &= v\left((\beta\delta v - \delta)(u+\alpha) - (u^2 + (v+\alpha-1)u - \alpha)\right). \end{aligned} \tag{3.1}$$

The upper hemisphere $Z > 0$ of the Poincaré sphere $X^2 + Y^2 + Z^2 = 1$ can be mapped onto the uv-plane by the coordinate transformation $u = X/Z$, $v = Y/Z$. Its inverse is

$$X = \frac{u}{\sqrt{1+u^2+v^2}}, \quad Y = \frac{v}{\sqrt{1+u^2+v^2}}, \quad Z = \frac{1}{\sqrt{1+u^2+v^2}}. \tag{3.2}$$

Since the system (3.1) is polynomial in u and v, its pullback to the upper hemisphere of the Poincaré sphere can be rescaled so that it extends smoothly to the equator $X^2 + Y^2 = 1$, $Z = 0$. The equator of the Poincaré sphere correspond to the circle at infinity of the uv-plane [3].

In computations, typically two sets of affine coordinates are used:

$$(1)\ x = 1/u,\ y = v/u \text{ on } u \neq 0, \text{ and } (2)\ x = u/v,\ y = 1/v \text{ on } v \neq 0.$$

Using the rescaled flow in these coordinates, together with the flow of the original vector field (3.1), one can reconstruct the flow on the Poincaré sphere [3].

For $\delta > 1$, Figure 3.2 shows the flow of the pullback of (3.1) in the quadrant $X \geq 0,\ Y \geq 0$ of the Poincaré sphere, after rescaling. This quadrant of the Poincaré sphere corresponds to the quadrant $u \geq 0,\ v \geq 0$ for (3.1). The equilibria on the circle at infinity are labeled E, F, and G. F is a hyperbolic saddle, G is a hyperbolic attractor, and E is a nonhyperbolic equilbrium for which the displayed region in the first quadrant is a hyperbolic sector if $\beta\delta < 2$ and an attracting parabolic sector if $\beta\delta > 2$. The remainder of this section is devoted to justifying this description of the equilibria on the circle at infinity.

3.2. **The coordinate system $x = 1/u,\ y = v/u$.** We make the change of variables $x = 1/u,\ y = v/u$ in (3.1), and multiply the resulting vector field by x^2. The result is

$$\begin{aligned} x' &= -x - xy + (1-\alpha)x^2 + \alpha x^3, \\ y' &= (\beta\delta - 2)y^2 - 2y + (2 - 2\alpha - \delta)xy + \alpha\beta\delta xy^2 + (2\alpha - \delta)x^2 y. \end{aligned} \tag{3.3}$$

On the line $x = 0$ (which corresponds to the "line" $u = \infty$) there are equilibria at $y = 0$ and $y = 2/(\beta\delta - 2)$. The eigenvalues of the linearization of (3.3) at $(0,0)$ are -1 and -2, and the eigenvalues of the linearization of (3.3) at $(0, 2/(\beta\delta - 2))$ are $\beta\delta/(2 - \beta\delta)$ and 2. In Figure 3.2, $(0,0)$ corresponds to G and $(0, 2/(\beta\delta - 2))$ to F.

3.3. **The coordinate system $x = u/v,\ y = 1/v$.** We make the change of variables $x = u/v,\ y = 1/v$ in (3.1), and multiply the resulting vector field by y^2. The result is

$$\begin{aligned} x' &= (2 - \beta\delta)x^2 + 2x^3 + (2\alpha + \delta - 2)x^2 y - \alpha\beta\delta xy + (\delta - 2\alpha)xy^2, \\ y' &= (1 - \beta\delta)xy + x^2 y - \alpha\beta\delta y^2 + (\alpha + \delta - 1)xy^2 + \alpha(\delta - 1)y^3. \end{aligned} \tag{3.4}$$

On the line $y = 0$ (which corresponds to the "line" $v = \infty$) there are equilibria at $x = 0$ and $x = (\beta\delta - 2)/2$. The second of these equilbria corresponds to F in Figure 3.2 and has already been analyzed in the other coordinate system. The equilibrium at $(0,0)$ is degenerate: all partial derivatives of (3.4) there are 0. It corresponds to E in Figure 3.2.

3.4. **Analysis of the degenerate equilibrium.** We analyze the degenerate equilibrium $(0,0)$ of (3.4) using the polar coordinate map

$$\Phi : \mathbb{S}^1 \times \mathbb{R} \to \mathbb{R}^2, \quad ((\bar{x}, \bar{y}), r) \mapsto (x, y),$$

where $\bar{x}^2 + \bar{y}^2 = 1$ and

$$x = r\bar{x}, \quad y = r\bar{y}.$$

In computations, as in the previous subsections, typically two sets of affine coordinates are used:

$$(1)\ x = r,\ y = ry_1 \text{ on } x \neq 0, \text{ and } (2)\ x = rx_1,\ y = r \text{ on } y \neq 0.$$

Using the rescaled flow in these coordinates for small r, one can reconstruct the rescaled flow on $\mathbb{S}^1 \times \mathbb{R}$ for small r, and hence the flow of (3.4) near $(0,0)$.

In the coordinates $x = r,\ y = ry_1$, the system (3.4) becomes, after division by r:

$$\begin{aligned} \dot{r} &= (2 - \beta\delta)r + 2r^2 + (2\alpha + \delta - 2)r^2 y_1 - \alpha\beta\delta r y_1 + (\delta - 2\alpha)r^2 y_1^2, \\ \dot{y_1} &= -y_1 - ry_1 + ry_1^2 + (\alpha - \delta + \alpha\delta)ry_1^3. \end{aligned} \tag{3.5}$$

On the invariant line $r = 0$, (3.5) has the unique equilibrium $E_1 = (0,0)$ with eigenvalues $2 - \beta\delta$ and -1. It is therefore a saddle for $\beta\delta < 2$ and an attractor for $\beta\delta > 2$.

In the coordinates $x = rx_1,\ y = r$, the system (3.4) becomes, after division by r:

$$\begin{aligned} \dot{x_1} &= x_1^2 + rx_1^3 + (\alpha - 1)rx_1^2 + (\delta - \alpha - \alpha\delta)x_1 r, \\ \dot{r} &= (1 - \beta\delta)rx_1 + r^2x_1^2 - \alpha\beta\delta r + (\alpha + \delta - 1)r^2x_1 + \alpha(\delta - 1)r^2. \end{aligned} \tag{3.6}$$

On the invariant line $r = 0$, (3.6) has the unique equilibrium $E_2 = (0, 0)$ with eigenvalues 0 and $-\alpha\beta\delta$. A center manifold is the x_1-axis, on which the system reduces to $\dot{x_1} = x_1^2$.

Combining the results from the two coordinate systems, we obtain Figure 3.3, which shows the flow near the degenerate equilibrium $(0, 0)$ of (3.4) in polar coordinates. After blow-down we obtain either a hyperbolic sector or an attracting parabolic sector.

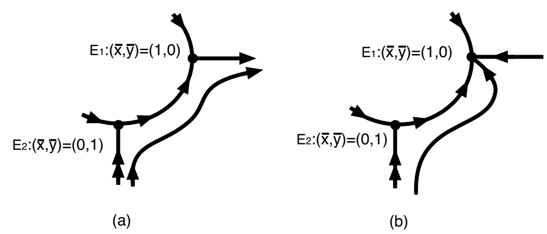

FIGURE 3.3. The flow near the degenerate equilibrium $(0, 0)$ of (3.4) in polar coordinates: (a) $\beta\delta < 2$, (b) $\beta\delta > 2$. So that the reader can more easily compare this figure with Figure 3.2, the circle $r = 0$ is shown upside down, with the point $(\bar{x}, \bar{y}) = (0, 1)$ at the bottom of the circle. With some abuse of notation, the equilibria are labeled E_1 and E_2 to correspond to the equilibria in the two affine coordinate systems.

References

[1] S. Ai, Y. Du, and R. Peng, Traveling waves for a generalized Holling-Tanner predator-prey model, J. Differential Equations, 263 (2017), 7782–7814.

[2] H. Cai, A. Ghazaryan, and V. Manukian, Fisher-KPP dynamics in diffusive Rosenzweig-MacArthur and Holling-Tanner models, Math. Model. Nat. Phenom., 14 (2019), Art. 404, 21 pp.

[3] C. Chicone, "Ordinary Differential Equations with Applications," 2nd edition, Springer Texts in Applied Mathematics 34, Springer, New York, 2006.

[4] N. Fenichel, Geometric singular perturbation theory for ordinary differential equations, J. Differential Eqs., 55 (1979), 763–783.

[5] A. Ghazaryan, V. Manukian, and S. Schecter, Traveling waves in the Holling-Tanner model with weak diffusion, Proc. A. 471 (2015), no. 2177, 20150045, 16 pp.

[6] A. Gasull, R. E Kooij, and J. Torregrosa, Limit cycles in the Holling-Tanner model, Publ. Mat., 41 (1997), 149–167.

[7] C. S. Holling, The characteristics of simple types of predation and parasitism, Canadian Entomologist, 91 (1959), 293–320.

[8] S.-B. Hsu and T.-W. Huang, Global stability for a class of predator-prey systems, SIAM J. Appl. Math, 31 (1995), 53–98.

[9] S.-B. Hsu and T.-W. Hwang, Uniqueness of limit cycles for a predator-prey system of Holling and Leslie type, Canad. Appl. Math. Quart., 6 (1998), 91–117.

[10] S.-B. Hsu and T.-W. Hwang, Hopf bifurcation analysis for a predator-prey system of Holling and Leslie type, Taiwanese J. Math., 3 (1999), 35–53.

[11] C. K. R. T. Jones, Geometric singular perturbation theory, in "Dynamical Systems (Montecatini Terme, 1994)," Lecture Notes in Math. 1609, Springer (1995).

[12] C. Kuehn, "Multiple Time Scale Dynamics," Springer, New York, 2015.

[13] X. Li, W. Jiang, and J. Shi, Hopf bifurcation and Turing instability in the reaction-diffusion Holling-Tanner predator-prey model, IMA J. Appl. Math., 78 (2013), 287–306.

[14] R. M. May, On relationships among various types of population models, American Naturalist, 107 (1973), 46–57.

[15] R. M. May, "Stability and Complexity in Model Ecosystems," Princeton University Press, Princeton, 1974.

[16] J. D. Murray, "Mathematical Biology," Springer, New York, 1989.

[17] E. Renshaw, "Modelling Biological Populations in Space and Time," Cambridge University Press, Cambridge, 1991.

[18] E. Sáez and E. González-Olivares, Dynamics of a predator-prey model, SIAM J. Appl. Math., 59 (1999), 1867–1878.

[19] J. T. Tanner, The stability and the intrinsic growth rates of prey and predator populations, Ecology, 56 (1975), 855–867.

[20] J. A. Sherratt and M. J. Smith, Periodic travelling waves in cyclic populations: field studies and reaction-diffusion models, J. R. Soc. Interface, 5 (2008), 483–505.

E-mail address: `manukive@miamioh.edu`

E-mail address: `schecter@ncsu.edu`